Universiti Malaysia Terengganu Journal of Undergraduate Research *eISSN: 2637-1138*
Volume 5 Number 3, July 2023: 51-64

MAPPING PADDY RICE EXTENT AND CROPPING PATTERN IN IADA BARAT LAUT SELANGOR USING INTEGRATION OF SENTINEL-1 AND SENTINEL-2 DATA

PHILIP WONG LIONG CHUN[1], SITI AISHAH SARUDIN[2], RUDIYANTO[1]*, NORHIDAYAH CHE SOH[1], RAMISAH MOHD SHAH[1], ROZAIDI ABDUL RAHMAN[2], EZZANA ABARSAH[2], AND MOHAMAD FIQRI SHAFFIE[2]

[1]Program of Crop Science, Faculty of Fisheries and Food Science, Universiti Malaysia Terengganu, 21030 Kuala Nerus, Terengganu, Malaysia. [2]IADA Barat Laut Selangor, Kompleks Pejabat IADA, 45000 Kuala Selangor, Selangor Darul Ehsan, Malaysia

**Corresponding author: rudiyanto@umt.edu.my* *https://doi.org/10.46754/umtjur.v5i3.381*

Abstract: Under the 12th Malaysia Plan (RMK-12), the Malaysian government has set a goal to achieve a self-sufficiency level (SSL) of 70% for rice production. Accurate and timely spatiotemporal information on harvested rice extent is required to measure progress towards achieving the SSL. Remote sensing technology has been widely used to provide rapid information on the extent of rice. This study aims to create maps of rice extent and cropping patterns in the IADA Barat Laut Selangor (BLS), combining Synthetic Aperture Radar (SAR) imagery data using Sentinel-1 and optical imagery data using Sentinel-2. The monthly composite data of VH polarization and the Normalized Difference Vegetation Index (NDVI) were stacked as bands in an imagery dataset, forming a time series dataset. The unsupervised K-means clustering method and the Google Earth Engine (GEE) cloud-based computing platform were used for the analysis of the data. The results allowed the classification of the rice and non-rice groups. The rice cropping patterns were generated from the temporal composites of VH backscatter values of Sentinel-1 data and NDVI of Sentinel-2 data. The map products were evaluated using accuracy measures using visual interpretation techniques applied to very high-resolution imagery acquired from Google Earth (GE). The rice extent map generated at 10-meter resolution exhibited excellent accuracy with an overall accuracy of 98% and a kappa coefficient of 0.95. The estimated rice parcel area in IADA BLS for 2021 was 17,864 ha, which is close to the recorded data (18,785 ha). The comparison of results in the irrigation block also indicated that the rice field area agreed well with the statistical data, with an R^2 of 0.95, RMSE of 357 ha, and a relative discrepancy of 4.9%. The cropping pattern also showed satisfactory results as compared to the existing data. These findings demonstrate that the proposed methodology can provide high-accuracy rice extent map products and has the potential to be applied to rice fields across Malaysia and other tropical regions to address food security issues. Subsequent investigations should prioritize addressing the challenge of detecting conversions into other land uses, which were not addressed in this study, by exploring alternative data sources, advanced machine learning algorithms, and incorporating ground-based surveys.

Keywords: Paddy rice fields, cropping calendar, food security, Google Earth Engine (GEE), Sentinel-1, Sentinel-2 surface reflectance.

Introduction

Rice is a staple food in Malaysia. Rice consumption in Malaysia increases yearly and is projected to reach 3.5 million MT in 2026 (Che Omar *et al*., 2019). Meanwhile, the production is estimated to be 2 million MT where out of this (2 million MT or 74.1% of the total rice produced) would be from the granary areas such as Muda Agricultural Development Authority (MADA), Kemubu Agricultural Development Authority (KADA) and Integrated Agricultural Development Area (IADA) Barat Laut Selangor (BLS), IADA Pulau Pinang, IADA Ketara, IADA Pekan and Rompin (Che Omar *et al*., 2019). To address the issue of food security,

the Malaysian government has established a target of achieving a self-sufficiency level (SSL) of 70% for local rice production under the 12th Malaysia Plan (RMK-12) (Ministry of Agriculture and Food Industries, 2011). To measure the achievement of the target, accurate and up-to-date spatiotemporal information on rice is necessary.

To provide spatiotemporal paddy rice area, remote sensing technology has emerged as a valuable tool, offering several advantages over field surveys. Unlike field surveys, which can be time-consuming, costly, and limited in coverage and frequency, remote sensing which has been used for more than two decades (Zhao *et al*., 2021), provides a rapid and timely means to generate maps of rice extent in large areas (Kuenzer & Knauer, 2013; Dong & Xiao, 2016). Synthetic Aperture Radar (SAR) Sentinel-1 and multispectral optical Sentinel-2 satellites were launched by the European Space Agency (ESA) on April 3, 2014 (The European Space Agency, n.d.-a; Torres *et al*., 2012) and June 23, 2015 (The European Space Agency, n.d.-b), respectively and its data are available in the public domain freely, the use of remote sensing for mapping high-resolution rice extent have been raised significantly (Nguyen *et al*., 2016). Another factor that both satellite imagery data are suitable for is mapping rice extent. It is a short revisit time that can capture rice phenology (Rudiyanto *et al.,* 2019; Fatchurrachman *et al.,* 2022). Constellation between Sentinel-2A and B results have a revisit time of 5 days at the equator (Shang & Zhu, 2019; Li & Chen, 2020). Meanwhile, Sentinel-1 has a revisit time of 12 days (Torres *et al*., 2012).

Sentinel-1 provides dual-polarized (VV + VH) SAR images that are acquired from the C-band (centre frequency: 5.405 GHz) radar sensor (Torres *et al*., 2012; Mullissa *et al*., 2021). Although the Sentinel-1 data is independent from the cloud, it contains speckle noise which is a type of random noise created by the interference between multiple echoes from different parts of the target in SAR images (Son *et al*., 2018). This noise can have an impact on data classification, particularly due to the presence of salt-and-pepper noise. Such noise can result in misclassification or reduced accuracy in the classification results, especially for small or complex features (Velasco *et al*., 2021).

Sentinel-2 provides high-resolution spatial imagery with 10 m and multi-spectral imagery in 13 spectral bands, covering a range of visible and near-infrared (NIR) wavelengths (Shang & Zhu, 2019). There are two types of Sentinel-2 products, namely Sentinel-2 Level 1C (Top of Atmosphere, TOA) and Level 2A (Surface Reflectance, RS) (The European Space Agency, n.d.-b). By comparison, mostly Sentinel-2 Level 1C (Top of Atmosphere, TOA) data were integrated with Sentinel-1 for mapping rice fields because the surface reflectance (SR) data was incomplete (Ni *et al*., 2021). As a result, the application of Sentinel-2 Level 2A for rice mapping is still limited.

This study aims to map rice extent and cropping calendar using a combination of Sentinel-1 and Sentinel-2 level 2A (SR) time series data in IADA BLS, which is known as one of the important granaries with high-yielding growth performance. IADA BLS contributes 8.1% of the total national rice production. Monthly VH polarization and NDVI composite imagery data of Sentinel-1 and Sentinel-2 SR, respectively, were stacked and used as input in the K-Means unsupervised method for classifying rice fields. Subsequently, the rice cropping calendar was generated based on the spectral profile of both VH polarization and NDVI time series data.

Materials and Methods

Study Area

The study area is in IADA Barat Laut Selangor (BLS) (Figure 1), located in the coastal plains of Sabak Benam and Kuala Selangor districts in the State of Selangor, Malaysia. The rectangular region of interest for this study area lies between 100.921°E to 101.283°E and 3.404°N to 3.765°N, covering 160,658 ha. IADA BLS region is divided into nine irrigation blocks

including Sawah Sempadan, Sungai Burong, Sekichan, Sungai Leman, Pasir Panjang, Sungai Nipah, Bagan Terap, Pancang Bedena, and Sungai Panjang (IADA Barat Laut Selangor, n.d.). In this study, Sungai Panjang is combined with Pancang Bendena and named Pancang Bedena.

The study area has a typically humid tropical climate, with the effects of monsoons in the northeast and southwest resulting in rainy seasons between October and December and between March and May, respectively (Suhaila *et al*., 2010). This has led to a bimodal rainfall pattern, with as much as 70% of the rainfall occurring during these two seasons. The average annual rainfall ranges between 1500 mm and 2000 mm (Houma *et al*., 2021). The period between June and August is typically dry.

Rice Cultivation Practices

The irrigation management system made rice fields in the area have two cropping seasons namely; the main season (planted in July to October) and the off-season (January to April). Various popular rice varieties are planted in the study area such as MR220 CL2 (which can take 97-113 days for harvest) (Muda Agriculture Development Authority (MADA), n.d.) which is planted in IADA BLS, constituting over 80%; MR263 (102-112 days) (Hashim, 2015), MR219 (104-111 days) (Ramli, 2015), and MR220 (104-118 days) (Ansori & Abdul Rahman, 2021). On a monthly basis, these rice varieties can be harvested around four months after planting and their phenology can be categorised into four stages including transplanting, vegetative, generative, and maturity stages, where every stage takes a 1 month (Rudiyanto *et al*., 2019).

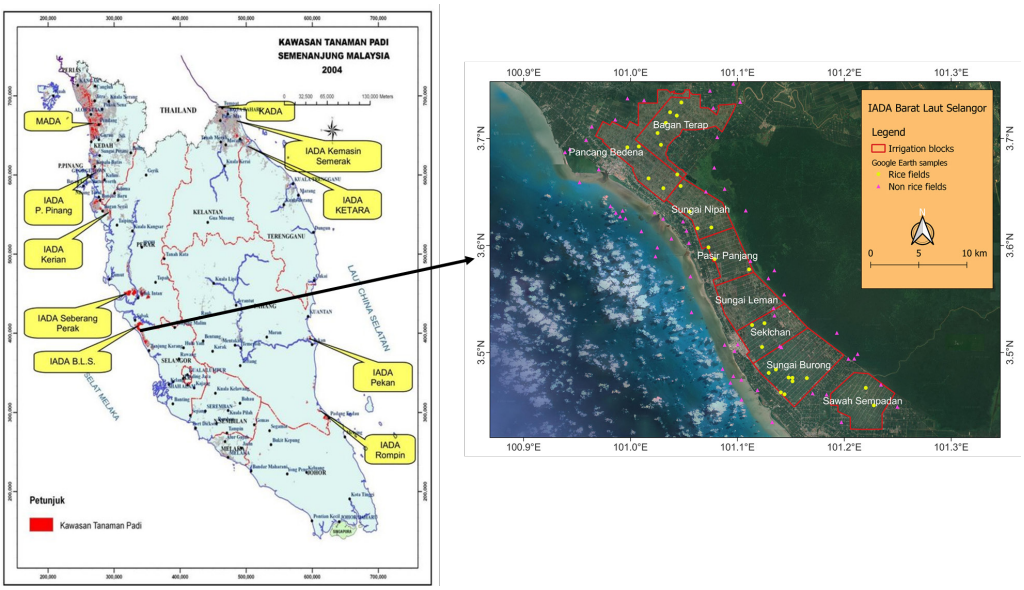

Figure 1: Maps showing the location of the granary area in Peninsular Malaysia (left) (Abu Bakar *et al*., 2020) and the study area in IADA Barat Laut Selangor (BLS), overlaid with irrigation blocks (right)

Sentinel-1 and Sentinel-2 Imagery Data

The Sentinel-1 Ground-Range-Detected (COPERNICUS/S1_GRD) is typically a calibrated and ortho-corrected product and the Harmonized Sentinel-2 Level-2A, a harmonized collection of an orthorectified Surface Reflectance (SR) product (COPERNICUS/S2_SR_HARMONIZED) from the data catalogue of Google Earth Engine (GEE) were used in this study. Both satellite imagery data have a 10 m spatial resolution. It notes that only sentinel-1A data was available in the study area, while Sentinel-1B is unavailable. On the other hand, both Sentinel-2A and 2B were available in the study area. Hereafter, Sentinel-2 was used for the term Sentinel-2A and 2B SR.

A total of 100 scenes of Sentinel-1A and 142 scenes of Sentinel-2A and 2B that covered the study area from January to December 2021 were collected from the data catalogue of GEE. These scenes were obtained from ascending and four descending orbit footprints for Sentinel-1 and two footprints of tiles for Sentinel-2A and 2B.

Although Sentinel-1 data consists of VH and VV polarization, only VH polarization was used in this study since it has higher sensitivity than VV polarization data for mapping rice fields (Nguyen *et al*., 2016; Rudiyanto *et al*., 2019). Sentinel-2 data comprises 13 bands; however, only two bands; band 4 (Red) and band 8 (NIR), were used in this study since they could be used to generate Normalized Difference Vegetation Index (NDVI) which is calculated by (Montero *et al*., 2023):

$$NDVI = \frac{(\text{band 8 (NIR)} - \text{band 4 (Red)})}{(\text{band 8 (NIR)} + \text{band 4 (Red)})} \quad (1)$$

In this study, VH polarization will be used to detect the presence of standing water during soil tillage or transplanting. Meanwhile, NDVI would be used to capture green and senescence during rice growth.

Methods

The methodology used in this study for mapping the extent of rice fields and the cropping schedule is depicted in Figure 2 and was implemented through GEE. The procedure involved the following steps:

Filtering Sentinel-1 and Sentinel-2 Datasets

The data in the image collection of GEES were loaded and then filtered by date range and region of interest (ROI) as bounds. Time series data in the ROI was obtained from these filtered datasets.

Generating Monthly Composite Imagery

For the Sentinel-1 dataset, monthly median composite data was generated to reduce speckle and border noise (Rudiyanto *et al*., 2019), while monthly maximum NDVI was generated from Sentinel-2 data to minimize the effect of the cloud (Holben, 1986). This composite of Sentinel-1 and Sentinel-2 data can solve the problem of different image acquisition times (Fatchurrachman *et al*., 2022). Moreover, it can also align the Sentinel-1 and 2 data with the stages of rice growth outlined in the Rice Cultivation section (Fatchurrachman *et al*., 2022). A total of 12 monthly median VH polarization data of Sentinel-1 and 12 monthly maximum NDVI data from Sentinel-2 were generated from a year's data and subsequently stacked into 24 bands of an image with 10 m spatial resolution. All these processes were done using GEE which employed nearest neighbor resampling by default during transformation.

Clustering

The unsupervised K-Means clustering method was employed to cluster the stacked image because it offers several advantages. It is relatively simple to implement, can manage large data sets, ensures convergence, allows for warm starting of the centroids' positions, easily adapts to new examples, and generalizes well to clusters of various shapes and sizes, including elliptical clusters. The method automatically normalized the training data as input and

updated the centroids of the clusters based on the Euclidean distance and the number of clusters iteratively. Once the centroids of the clusters were obtained, they were applied to all pixels, resulting in a specific number of clusters. A total of 2,000 random points were sampled in the area and then used as input in the K-Means method to generate 20 clusters. It is assumed that this number of clusters was sufficient to describe the variance of the input data (Rudiyanto *et al*., 2019). The remaining parameters for the K-means clustering method were set to their default values in GEE.

Extracting Profile Spectra for Each Cluster

After forming the pixel clusters, we extracted representative monthly spectra time series for each cluster. These time series consisted of VH polarization and NDVI values and were obtained by aggregating the spatial median value from a random sample of 2,000 points. The aggregation process over space was performed using the 'ee. Reducer.median' function in GEE.

Labelling and Classifying Rice Extent

The profile spectra time series of VH polarization and NDVI data were visually inspected to classify clusters as either rice or non-rice fields (water body, built-up, forest tree, and other vegetation) based on the unique characteristics of rice fields, including the presence of water during transplanting and rapid green-up during vegetative stages and senescence during maturity (Rudiyanto *et al.,* 2019; Fatchurrachman *et al.,* 2022).

Identifying Rice Patterns and Calendar

A rice calendar was established through the analysis of different schedules for rice planting seasons, as indicated by profile spectra time series data from VH polarization and NDVI measurements. Upon identification of the transplanting stage, it becomes simpler to distinguish the following phases: vegetative, generative and maturity (Rudiyanto *et al.,* 2019; Fatchurrachman *et al.,* 2022) .

Accuracy Assessments

The accuracy assessment of the produced maps in this study involved three types of evaluation. Firstly, validation was conducted using virtual observations based on Google Earth's VHR (remarkably high resolution) and street-view images. Secondly, a comparison was made with the rice parcel area released by the Malaysian Remote Sensing Agency (MRSA). Lastly, a comparison was made with the known planting and harvesting schedule provided by IADA BLS.

For the first assessment, 100 random points were generated within the study area (Figure 1). Each location was manually evaluated based on VHR images from the year 2020 and Google Earth Street view images. Among the 100 points, 33 were identified as rice fields, while 67 points were classified as non-rice areas. The accuracy of the rice maps was then evaluated using the confusion matrix and Kappa value based on this virtual field data.

A scattering plot was generated to facilitate the comparison of the rice parcel area and the evaluation was based on the R^2 and RMSE values. Furthermore, the relative discrepancy was employed to compare the rice parcel area at the block level between this study and the MRSA data. Additionally, a comparison of the cropping calendar was conducted between the results obtained in this study and the schedule provided by IADA BLS, focusing on the level of irrigation block.

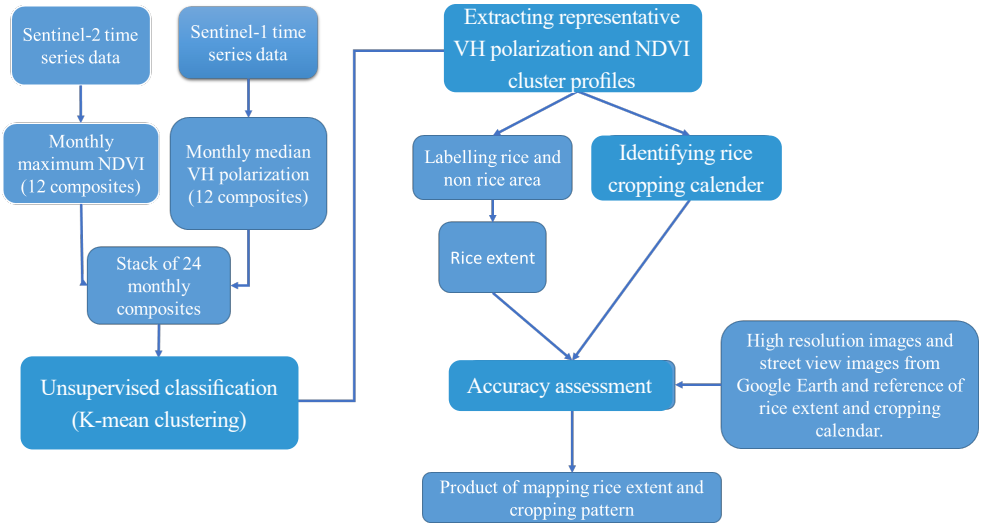

Figure 2: Workflow of the method for mapping rice extent and cropping calendar

Results and Discussion

Temporal Profiling VH Polarization and NDVI of Paddy Rice Fields

Out of 20 clusters, five clusters were identified as rice fields, one as waterbody, two as built-up and 12 as non-rice vegetation. Figures 3(a) and Figures 3(c) show the representative temporal profiles of VH polarization and NDVI for paddy rice fields, waterbody, built-up, and non-rice vegetation. Waterbodies exhibit a consistent VH polarization of around -27 dB due to the smooth surfaces reflecting SAR signals via specular reflection (Singha *et al*., 2019) and NDVI at 0.02. Non-rice vegetation exhibits relatively constant high values of VH polarization at -15 dB and NDVI at 0.8. Built-up areas can be distinguished by relatively high values of VH polarization at -14 dB due to the double-bounce effect (Son *et al*., 2021), while their NDVI values remain relatively constant at 0.2. The temporal profile of rice fields exhibits a unique spectrum, where VH polarization and NDVI are low during transplanting at around -22 and 0.2, respectively and increase rapidly during the vegetative stage at -19 for VH polarization and 0.75 for NDVI. During the maturity stage, its NDVI drops to 0.5 while its VH polarization remains high at -16, similar to built-up and non-rice vegetation. The rice phenology extracted from temporal profiles of VH polarization and NDVI can be found in Figures 3(b) and Figures 3(d), respectively. It shows that one season takes four months which is in line with the length of the rice growth period described in Section Rice cultivation practices.

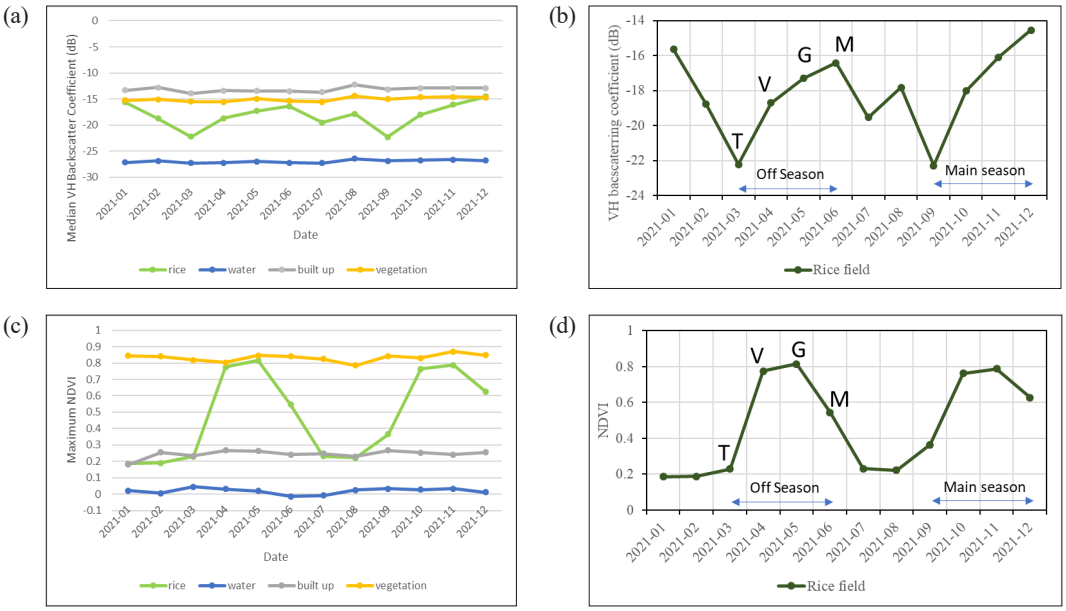

Figure 3: Profiles of temporal (a) VH polarization and (b) NDVI for paddy rice fields, waterbodies, built-up areas and non-rice vegetation from January to December 2021. Extraction of rice phenology from profiles of temporal (a) VH polarization and (b) NDVI, where T, V, G, and M represent the transplanting, vegetative, generative, and maturity stages, respectively

Map Product of Paddy Rice Extent

Figure 4 depicts the extent of paddy rice production at IADA BLS for 2021 overlaid with the irrigation block. The accuracy assessment, comparing the extracted pixel level of 100 points on the map product to high-resolution images and street view images in Google Earth, indicates excellent results, as presented in Table 1. The overall accuracy and kappa coefficient are 98% and 0.95, respectively. These findings are consistent with Rudiyanto *et al*. (2019) previous study, which used Sentinel-1 to map rice extent in MADA Kedah and reported an overall accuracy of 98% with a kappa coefficient of 0.94. In addition, Fatchurrachman *et al*. (2022) study, which used the integration of Sentinel-1 and 2 Level 1C to map rice extent across Peninsular Malaysia reported similar results, with an overall accuracy of 95% and a kappa coefficient 0.92. Misclassification often occurs at the boundary between rice fields and non-rice areas (around road and canal areas) due to mixed-pixel problems, as discussed in previous studies (Rudiyanto *et al.,* 2019; Son *et al.,* 2021; Fatchurrachman *et al.,* 2022).

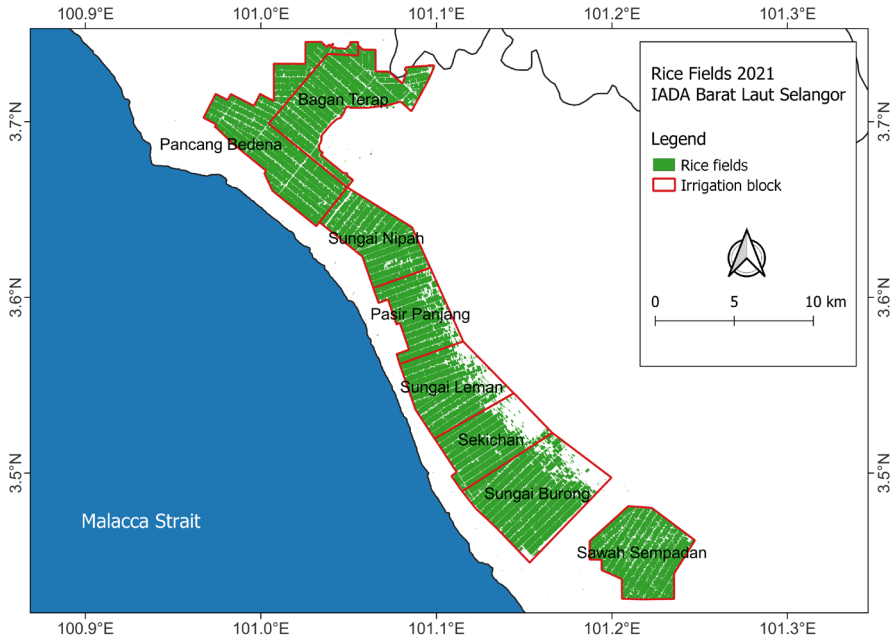

Figure 4: Map of rice fields in IADA BLS for 2021 derived from this study, overlaid with irrigation blocks

Table 1: Confusion matrix, overall accuracy and kappa value for the classification of rice fields in this study

		Predicted Class			Producer Accuracy	
		Non-Rice	**Rice**	**Total**	**Percent Correct**	**Omission Error (%)**
Reference Class	Non-rice	67	0	67	100.0	0.0
	Rice	2	31	33	93.9	6.1
	Total	**69**	**31**	**100**		
User accuracy						
Percent correct		97.1	100.0		**98.00**	
Commission error (%)		2.9	0.0			
Kappa value		**0.95**				

Apart from evaluating the positional accuracy, an extra validation was conducted at the total area and irrigation block level to compare the mapping results with the existing data from Sistem Geospatial Padi by the Malaysian Remote Sensing Agency, as released by the IADA BLS agency (IADA Barat Laut Selangor, n.d.) and satellite-based estimates of the rice-parcel area to ensure their coherence. Table 2 compares the rice parcel area for 2021 derived from this study with the existing data. The total rice parcel area in this study is 17,864 ha, comparable to the existing data (18,785 ha) with a discrepancy of 4.9%.

When comparing the extracted area of rice fields in the level irrigation blocks, the estimates in this study are generally lower than existing data, except for Bagan Terap and Sungai Panjang. The percentage discrepancies ranged between -1.13% and 14.45%. The largest discrepancy is found in Sungai Burong, which has a relatively large area of non-rice

vegetation, as shown in Figure 4. The dynamic conversion of rice fields may have influenced this discrepancy, as shown in Sungai Leman and Pasir Panjang. However, since the existing data is only available in numeric format, a map-to-map comparison cannot be performed to identify the specific locations with different results.

Table 2: Comparison of rice extent for 2021 in IADA BLS between this study and Sistem Geospatial Padi from the Malaysian Remote Sensing Agency (MRSA), along with their relative discrepancies

Irrigation Block	Rice Extent for 2021 (ha)		Relative Discrepancy (%)
	This Study	Sistem Geospatial Padi MRSA	
Sawah Sempadan	2,270	2,294	1.05
Sungai Burong	2,872	3,357	14.45
Sekichan	1,569	1,593	1.51
Sungai Leman	1,827	2,023	9.69
Pasir Panjang	1,444	1,585	8.90
Sungai Nipah	1,897	1,923	1.35
Bagan Terap and Sungai Panjang	2,765	2,734	-1.13
Pancang Bedena	3,220	3,276	1.71
Total	**17,864**	**18,785**	**4.90**

Figure 5 presents a correlation analysis that evaluated the agreement between the mapping results and existing data at the irrigation level. The analysis shows a strong linear relationship, with a coefficient of determination (R^2) of 0.95 and an RMSE of 357 ha.

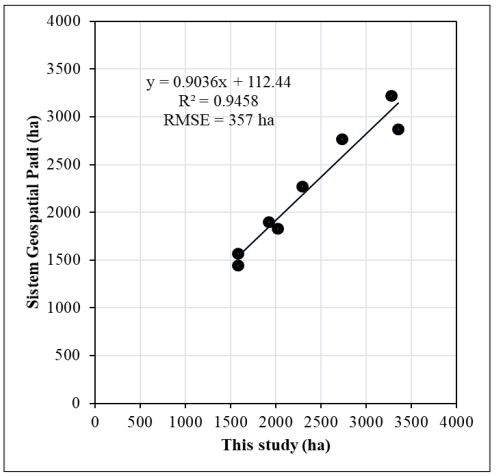

Figure 5: Correlation between rice extent estimates for 2021 derived from this study and Sistem Geospatial Padi by the Malaysian Remote Sensing Agency

Map Product of Paddy Rice Cropping Calendar

Five clusters of rice fields were identified and their temporal profile spectra of VH polarization and NDVI data are shown in Figures 6(b) and Figures 6(c). Four rice cropping patterns for 2021 were identified, namely Rice-1, Rice-2, Rice-3, and two clusters identified as Rice-4, corresponding to the rice field area shown in Figure 6(a). Based on Figure 3, the rice phenology for the four different rice patterns was extracted from Figures 6(b) and Figures 6(c) and summarized in Table 3. During the off-season, Rice-1 planted in January can be found at Sawah Sempadan, while Rice-2 planted in February, is located at Sungai Borong. Rice-3, planted in March, can be found at Sekichan, Sungai Leman, Pasir Panjang, and Sungai Nipah. Rice-4 planted in April, is located at Bagan Terap and Pancang Bedena. For the main season, Rice-1 planted in July, can be found at Sawah Sempadan, while Rice-2 planted in August, is located at Sungai Borong. Rice-3, planted in September, can be found at Sekichan, Sungai Leman, Pasir Panjang, and Sungai Nipah. The Rice-4 planted in October is located at Bagan Terap and Pancang Bedena. These findings are consistent with the IADA BLS data presented in Table 3.

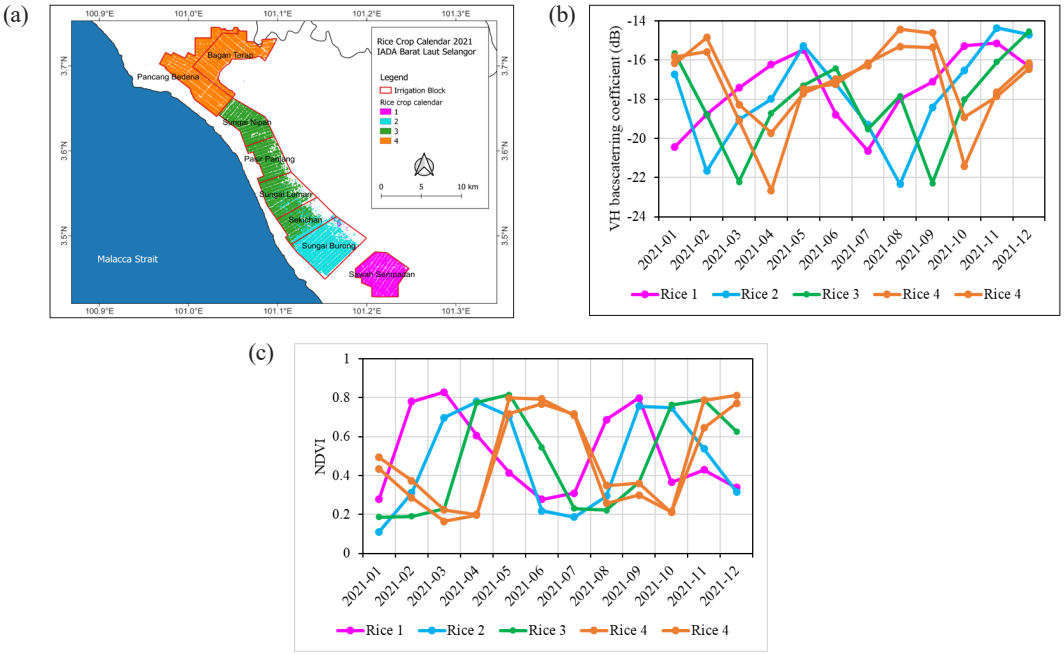

Figure 6: (a) Map of rice field cropping patterns for 2021, corresponding to profiles of temporal (b) VH polarization, and (c) NDVI data for rice groups 1, 2, 3, and 4; and cropping calendar in Table 3

Table 3: Comparison of rice cropping calendar between this study and IADA BLS data for 2021. The main season is from July to December 2021, while the off-season is from January to July 2021. The symbols T, V, G, and M represent the transplanting, vegetative, generative, and maturity stages, respectively

Rice Pattern	Irrigation Block	Jan-21	Feb-21	Mar-21	Apr-21	May-21	Jun-21	Jul-21	Aug-21	Sep-21	Oct-21	Nov-21	Dec-21
IADA BLS Data													
1	Sawah Sempadan	T	V	R	M			T	V	R	M		
2	Sungai Burong		T	V	R	M			T	V	R	M	
3	Sekichan, Sungai Leman, Pasir Panjang and Sungai Nipah			T	V	R	M			T	V	R	M
4	Pancang Bedena, Bagan Terap and Sungai Panjang	M			T	V	R	M			T	V	R
This Study													
1	Sawah Sempadan	T	V	R	M			T	V	R	M		
2	Sungai Burong		T	V	R	M			T	V	R	M	
3	Sekichan, Sungai Leman, Pasir Panjang and Sungai Nipah			T	V	R	M			T	V	R	M
4	Pancang Bedena, Bagan Terap and Sungai Panjang	M			T	V	R	M			T	V	R

Temporal Harvested Rice Area

Figure 7 presents the temporal harvested rice cultivation area in IADA BLS for 2021, which was derived from the rice calendar shown in Table 3, and the spatial distribution of the cropping calendar in Figure 6(a). The highest harvested rice area, of approximately 6,000 hectares, occurred in January, June, July, and December 2021. In contrast, no harvested rice area was recorded during February, March, August, and September 2021.

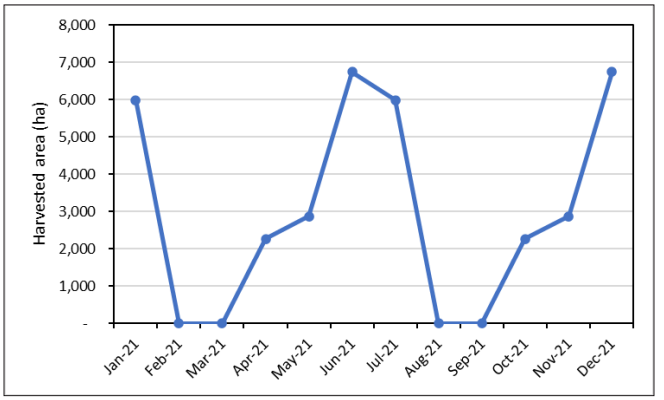

Figure 7: Temporal harvested rice cultivation area in IADA BLS for 2021

Limitations of the Study

The unsupervised clustering method with a phenology-based approach, which was implemented in this study can only capture the double rice intensity of rice fields in a year. If a rice field is converted into other land covers, such as other crops, built-up areas, or fallow land, during either the off or main season and the rice field becomes a single cropping calendar, the method cannot detect these changes. One approach to detecting changes in a time series data that spans one year is to reduce it to a single season. This can help to facilitate analysis and identify seasonal patterns (Jiang *et al*., 2022).

Conclusion

The combination of Sentinel-1, Sentinel-2 Level 2A, the unsupervised K-Means clustering method and Google Earth Engine (GEE) provides a simple and robust methodology that can result in high spatial resolution (10 m) and accurate maps of not only rice extent but also cropping calendars, rapidly. This approach can be implemented in other granary areas in Malaysia and the results can serve as a complementary source of information to other analytical data. Future research can extend the use of the generated mapped product to develop predictive models for paddy rice yield, significantly enhancing the study's outcomes. Furthermore, incorporating additional multispectral sensor data, such as Soil-Adjusted Vegetation Index (SAVI) and leaf area index (LAI), along with time series analysis, holds promise for improving the detection of rice diseases. Ultimately, the resulting product can serve as a crucial tool for policymakers, facilitating decisions regarding the import and export of paddy rice grain, farmer subsidies, water management, and the preservation of rice fields against conversion to other land uses, all in the context of ensuring food security.

Acknowledgments

This study was supported by Talent and Publication Enhancement-Research Grant (TAPE-RG) Dana Penyelidikan Universiti Malaysia Terengganu (DP–UMT), TAPE RG/2020/Vot 55246/UMT.

References

Ansori, A. R., & Abdul Rahman, S. M. (2021). An assessment of rice seed quality at various physiological harvest maturity stages. *GADING Journal of Science and Technology* , *4*(1). https://ir.uitm.edu.my/id/eprint/46247/1/46247.pdf

Che Omar, S., Shaharudin, A., & Tumin, S. A. (2019). *The status of the paddy and rice industry in Malaysia*. Khazanah Research Institute.

Dong, J., & Xiao, X. (2016). Evolution of regional to global paddy rice mapping methods: A review. *ISPRS Journal of Photogrammetry and Remote Sensing*, *119*, 214–227. https://doi.org/https://doi.org/10.1016/j.isprsjprs.2016.05.010

Fatchurrachman, Rudiyanto, Soh, N. C., Shah, R. M., Giap, S. G. E., Setiawan, B. I., & Minasny, B. (2022). High-resolution mapping of paddy rice extent and growth stages across Peninsular Malaysia using a fusion of sentinel-1 and 2 time series data in Google Earth engine. *Remote Sensing*, *14*(8). https://doi.org/10.3390/rs14081875

Hashim, S. (2015). *Protection of new varieties of rice in Malaysia*. http://eapvp.org/files/report/docs/malaysia/04-5%20Country%20Report_Malaysia2.pdf

Holben, B. N. (1986). Characteristics of maximum-value composite images from temporal AVHRR data. *International Journal of Remote Sensing*, *7*(11), 1417–1434. https://doi.org/10.1080/01431168608948945

Houma, A. A., Kamal, M. R., Mojid, M. A., Abdullah, A. F. B., & Wayayok, A. (2021). Climate change impacts on rice yield of a large-scale irrigation scheme in Malaysia. *Agricultural Water Management*, *252*, 106908. https://doi.org/https://doi.org/10.1016/j.agwat.2021.106908

IADA Barat Laut Selangor. (n.d.). *Kawasan pembangunan pertanian bersepadu IADA Barat Laut Selangor*. Retrieved January 2, 2022, from https://iadabls.mafs.gov.my/

Jiang, X., Luo, S., Gao, S., Fang, S., Wang, Y., Yang, K., Xiong, Q., & Li, Y. (2022). An automatic rice mapping method based on constrained feature matching exploiting Sentinel-1 data for arbitrary length time series. *International Journal of Applied Earth Observation and Geoinformation*, *114*, 103032. https://doi.org/https://doi.org/10.1016/j.jag.2022.103032

Kuenzer, C., & Knauer, K. (2013). Remote sensing of rice crop areas. *International Journal of Remote Sensing*, *34*(6), 2101–2139. https://doi.org/10.1080/01431161.2012.738946

Li, J., & Chen, B. (2020). Global revisit interval analysis of landsat-8 -9 and sentinel-2A -2B data for terrestrial monitoring. *Sensors*, *20*(22). https://doi.org/10.3390/s20226631

Ministry of Agriculture and Food Industries. (2011). *Dasar agromakanan negara 2011–2020*. Ministry of Agriculture and Food Industries.

Montero, D., Aybar, C., Mahecha, M. D., Martinuzzi, F., Söchting, M., & Wieneke, S. (2023). A standardized catalogue of spectral indices to advance the use of remote sensing in Earth system research. *Scientific Data*, *10*(1), 197. https://doi.org/10.1038/s41597-023-02096-0

Muda Agriculture Development Authority (MADA). (n.d.). *New rice variety.* Retrieved February 16, 2023, from https://www.mada.gov.my/?page_id=13023&lang=en

Nguyen, D. B., Gruber, A., & Wagner, W. (2016). Mapping rice extent and cropping scheme in the Mekong Delta using Sentinel-1A data. *Remote Sensing Letters*, *7*(12), 1209–1218. https://doi.org/10.1080/2150704X.2016.1225172

Ni, R., Tian, J., Li, X., Yin, D., Li, J., Gong, H., Zhang, J., Zhu, L., & Wu, D. (2021). An enhanced pixel-based phenological feature for accurate paddy rice mapping with sentinel-2 imagery in Google Earth

Engine. *ISPRS Journal of Photogrammetry and Remote Sensing*, *178*, 282–296. https://doi.org/https://doi.org/10.1016/j.isprsjprs.2021.06.018

Ramli, A. (2015). *Rice breeding, production and distribution of rice in Malaysia.* MARDI. http://eapvp.org/files/report/docs/malaysia/04-4%20Country%20Report_Malaysia1.pdf

Rudiyanto, Minasny, B., Shah, M. R., Soh, N. C., Arif, C., & Setiawan, B. I. (2019). Automated near-real-time mapping and monitoring of rice extent, cropping patterns, and growth stages in Southeast Asia using sentinel-1 time series on a Google Earth Engine Platform. *Remote Sensing, 11*(14), 1666. https://doi.org/10.3390/rs11141666

Shang, R., & Zhu, Z. (2019). Harmonizing landsat 8 and sentinel-2: A time-series-based reflectance adjustment approach. *Remote Sensing of Environment*, *235*, 111439. https://doi.org/https://doi.org/10.1016/j.rse.2019.111439

Singha, M., Dong, J., Zhang, G., & Xiao, X. (2019). High resolution paddy rice maps in cloud-prone Bangladesh and Northeast India using sentinel-1 data. *Scientific Data*, *6*(1), 26. https://doi.org/10.1038/s41597-019-0036-3

Son, N.-T., Chen, C.-F., Chen, C.-R., & Minh, V.-Q. (2018). Assessment of Sentinel-1A data for rice crop classification using random forests and support vector machines. *Geocarto International*, *33*(6), 587–601. https://doi.org/10.1080/10106049.2017.1289555

Son, N.-T., Chen, C.-F., Chen, C.-R., Toscano, P., Cheng, Y.-S., Guo, H.-Y., & Syu, C.-H. (2021). A phenological object-based approach for rice crop classification using time-series Sentinel-1 Synthetic Aperture Radar (SAR) data in Taiwan. *International Journal of Remote Sensing*, *42*(7), 2722–2739. https://doi.org/10.1080/01431161.2020.1862440

Suhaila, J., Mohd Deni, S., Wan Zin, W. Z., & Jemain, A. A. (2010). Trends in Peninsular Malaysia rainfall data during the southwest monsoon and northeast monsoons seasons: 1975-2004. *Sains Malaysiana*, *39*(4), 533–542.

The European Space Agency. (n.d.-a). *Sentinel-1*. Retrieved February 15, 2023, from https://sentinels.copernicus.eu/web/sentinel/missions/sentinel-1

The European Space Agency. (n.d.-b). *Sentinel-2*. Retrieved February 15, 2023, from https://sentinels.copernicus.eu/web/sentinel/missions/sentinel-2

Torres, R., Snoeij, P., Geudtner, D., Bibby, D., Davidson, M., Attema, E., Potin, P., Rommen, B., Floury, N., Brown, M., Traver, I. N., Deghaye, P., Duesmann, B., Rosich, B., Miranda, N., Bruno, C., L'Abbate, M., Croci, R., Pietropaolo, A., … & Rostan, F. (2012). GMES Sentinel-1 mission. *Remote Sensing of Environment*, *120*, 9–24. https://doi.org/https://doi.org/10.1016/j.rse.2011.05.028

Velasco, A., Rabus, B., & Beg, M. F. (2021). Comparison of speckle noise filters on crop classification based on sentinel-1 sar time-series. *2021 IEEE International India Geoscience and Remote Sensing Symposium (InGARSS)*, 61–64. https://doi.org/10.1109/InGARSS51564.2021.9791938

Zhao, R., Li, Y., & Ma, M. (2021). Mapping paddy rice with satellite remote sensing: A review. *Sustainability*, *13*(2). https://doi.org/10.3390/su13020503